

# Near-threshold $J/\psi$ Photoproduction

Wen-Chen Chang

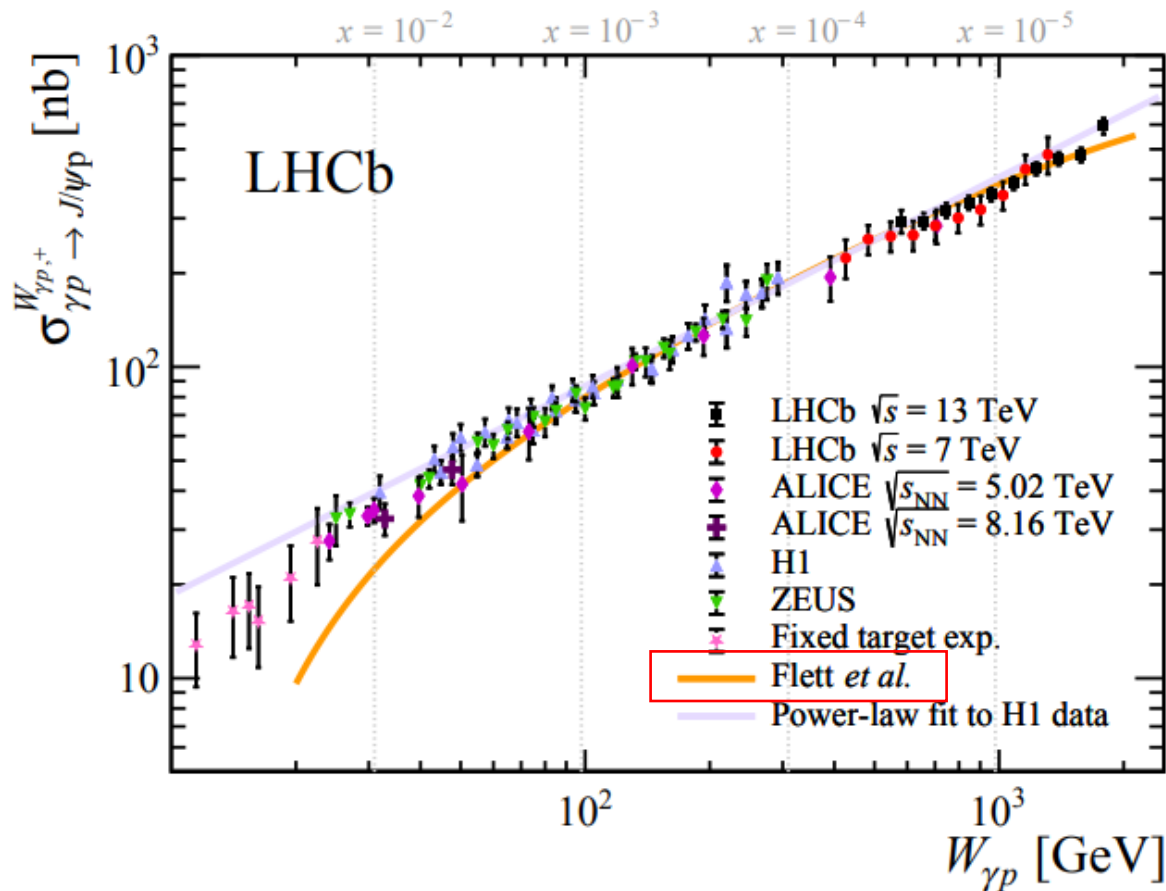
October 2, 2025

# References

- Exps:
  - <https://inspirehep.net/literature/1736890> (GlueX)
  - <https://inspirehep.net/literature/2110821> (007)
  - <https://inspirehep.net/literature/2649988> (GlueX)
- Theoretical works:
  - <https://journals.aps.org/prd/abstract/10.1103/PhysRevD.104.054015>
  - <https://journals.aps.org/prd/abstract/10.1103/PhysRevD.103.096010>
  - <https://link.springer.com/article/10.1140/epjc/s10052-020-08620-5>
  - <https://www.sciencedirect.com/science/article/pii/S0370269324004623>
  - <https://arxiv.org/abs/2210.02154> : providing a nice summary of theoretical models
  - <https://arxiv.org/abs/2403.01958>
- Talks:
  - <https://conferences.lbl.gov/event/2045/contributions/10907/attachments/5812/5978/CFR-2025-Berkeley.pdf>
  - [https://indico.ijclab.in2p3.fr/event/11650/attachments/25603/37726/SeminairePHE\\_JPsi\\_CLAS12\\_V2.pdf](https://indico.ijclab.in2p3.fr/event/11650/attachments/25603/37726/SeminairePHE_JPsi_CLAS12_V2.pdf)
  - [https://indico.phys.sinica.edu.tw/event/52/contributions/221/attachments/200/336/TIDC\\_EIC\\_Peng.pdf](https://indico.phys.sinica.edu.tw/event/52/contributions/221/attachments/200/336/TIDC_EIC_Peng.pdf)
- GFFs:
  - <https://arxiv.org/abs/2402.05354>
  - <https://arxiv.org/abs/2308.04644>
  - <https://arxiv.org/abs/2208.03186>

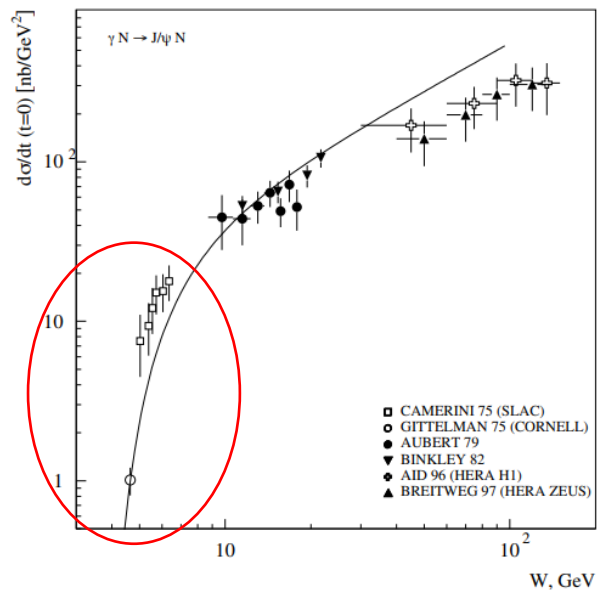
# Jpsi Photoproduction at high energies

$$x = \frac{M_{Jpsi}}{\sqrt{s}} e^{-y}$$



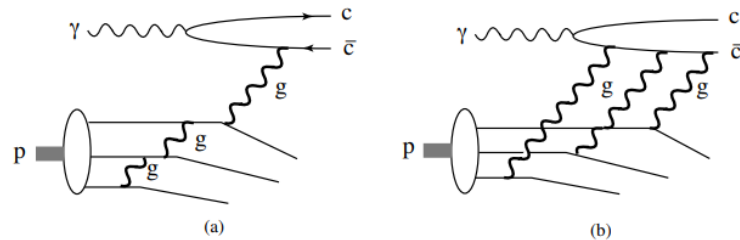
# Near-threshold $J/\psi$ Photoproduction - Before New Results from Jlab

## $J/\psi$ photoproduction (near threshold)



*Kharzeev et al. [EPJC 9 (1999) 459]*

*Brodsky et al. [PLB 498 (2001) 23]*



No other obviously contributing process:

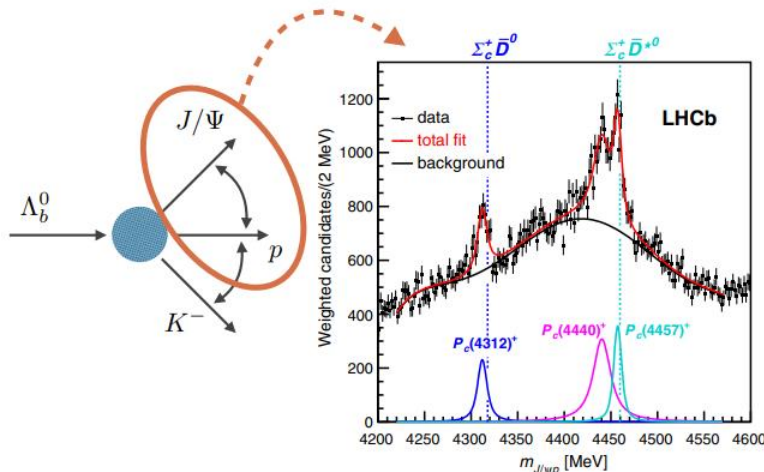
- Small  $J/\psi \rightarrow NN$  (no baryon exchanges)
- OZI suppression (no light meson exchanges)
- Heavy quark masses (no heavy meson exchanges)

" $J/\psi$  probes nonperturbative gluonic distributions"

# J/ψ-N Resonance Pc(4440)

## J/ψ photoproduction (near threshold)

Measurements at energies near threshold have attracted a lot of attention as potentially sensitive to key quantities relevant to **exotic hadrons**



These data: LHCb [PRL 122 (2019) 222001]

Discovery: LHCb [PRL 115 (2015) 072001]

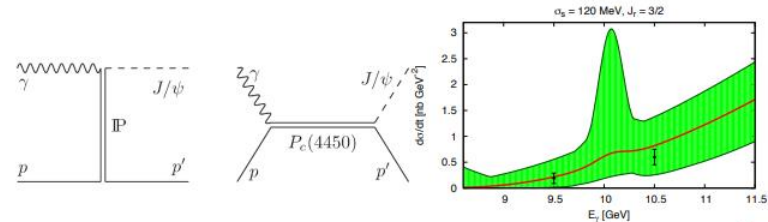
Prediction: Wu, Molina, Oset & Zou [PRL 105 (2010) 232001]

Observation of hidden charm pentaquark candidates by LHCb sparked interest in photoproduction searches

Wang et al. [PRD 92 (2015) 034022]

Karliner & Rosner [PLB 752 (2016) 329]

Hiller Blin et al. [PRD 94 (2016) 034002]



# GlueX: PRL 123, 072001 (2019)

## arXiv:1905.10811

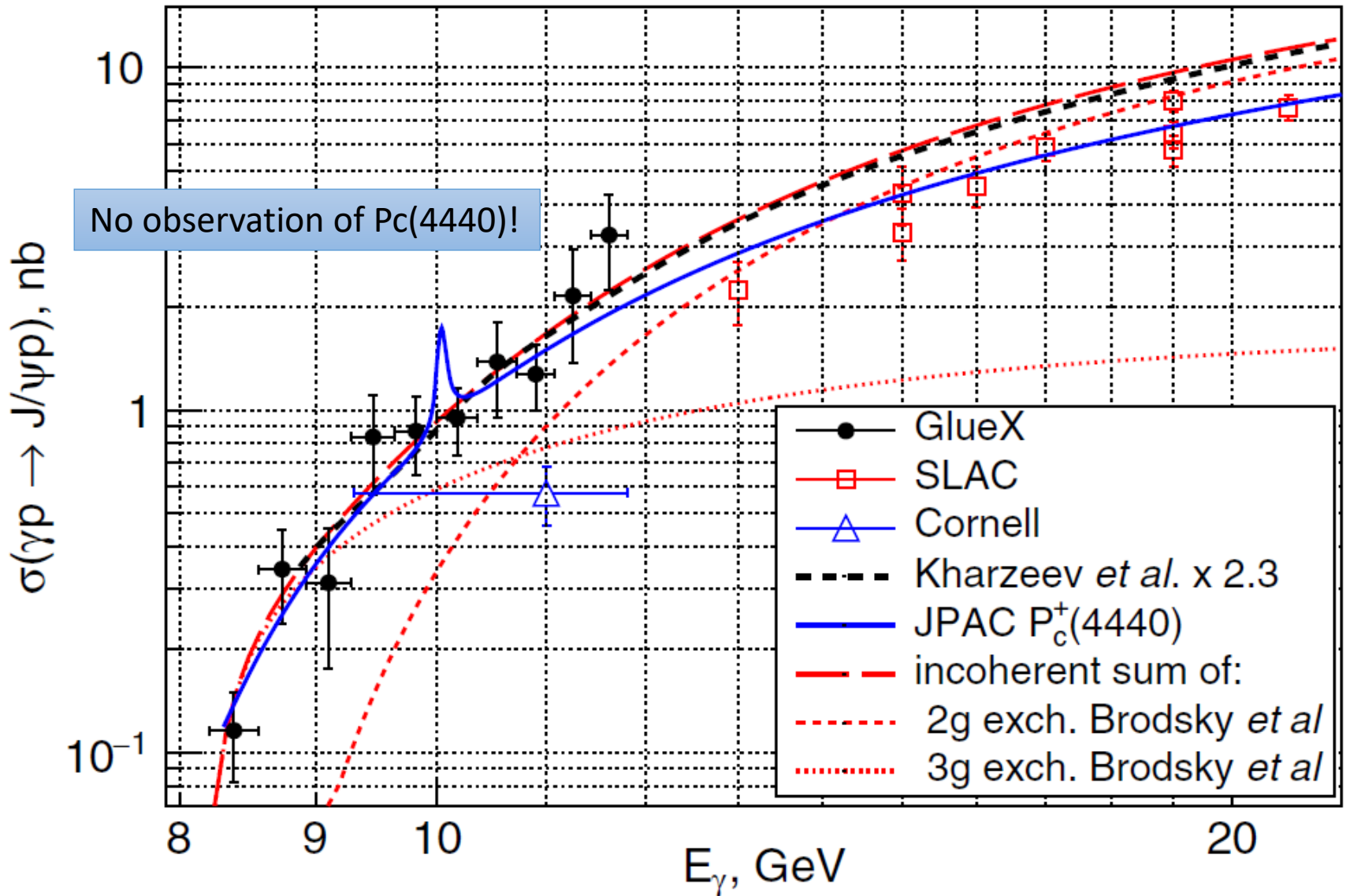
PHYSICAL REVIEW LETTERS **123**, 072001 (2019)

Editors' Suggestion

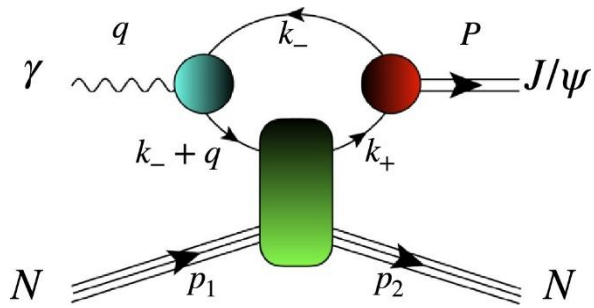
### First Measurement of Near-Threshold $J/\psi$ Exclusive Photoproduction off the Proton

A. Ali,<sup>10</sup> M. Amarian,<sup>22</sup> E. G. Anassontzis,<sup>2</sup> A. Austregesilo,<sup>3</sup> M. Baalouch,<sup>22</sup> F. Barbosa,<sup>14</sup> J. Barlow,<sup>7</sup> A. Barnes,<sup>3</sup> E. Barriga,<sup>7</sup> T. D. Beattie,<sup>23</sup> V. V. Berdnikov,<sup>17</sup> T. Black,<sup>20</sup> W. Boeglin,<sup>6</sup> M. Boer,<sup>4</sup> W. J. Briscoe,<sup>8</sup> T. Britton,<sup>14</sup> W. K. Brooks,<sup>24</sup> B. E. Cannon,<sup>7</sup> N. Cao,<sup>11</sup> E. Chudakov,<sup>14</sup> S. Cole,<sup>1</sup> O. Cortes,<sup>8</sup> V. Crede,<sup>7</sup> M. M. Dalton,<sup>14</sup> T. Daniels,<sup>20</sup> A. Deur,<sup>14</sup> S. Dobbs,<sup>7</sup> A. Dolgolenko,<sup>13</sup> R. Dotel,<sup>6</sup> M. Dugger,<sup>1</sup> R. Dzhygadlo,<sup>10</sup> H. Egiyan,<sup>14</sup> A. Ernst,<sup>7</sup> P. Eugenio,<sup>7</sup> C. Fanelli,<sup>16</sup> S. Fegan,<sup>8</sup> A. M. Foda,<sup>23</sup> J. Foote,<sup>12</sup> J. Frye,<sup>12</sup> S. Furletov,<sup>14</sup> L. Gan,<sup>20</sup> A. Gasparian,<sup>19</sup> V. Gauzshtein,<sup>25,26</sup> N. Gevorgyan,<sup>27</sup> C. Gleason,<sup>12</sup> K. Goetzen,<sup>10</sup> A. Goncalves,<sup>7</sup> V. S. Goryachev,<sup>13</sup> L. Guo,<sup>6</sup> H. Hakobyan,<sup>24</sup> A. Hamdi,<sup>10</sup> S. Han,<sup>29</sup> J. Hardin,<sup>16</sup> G. M. Huber,<sup>23</sup> A. Hurley,<sup>28</sup> D. G. Ireland,<sup>9</sup> M. M. Ito,<sup>14</sup> N. S. Jarvis,<sup>3</sup> R. T. Jones,<sup>5</sup> V. Kakoyan,<sup>27</sup> G. Kalicy,<sup>4</sup> M. Kamel,<sup>6</sup> C. Kourkouvelis,<sup>2</sup> S. Kuleshov,<sup>24</sup> I. Kuznetsov,<sup>25,26</sup> I. Larin,<sup>15</sup> D. Lawrence,<sup>14</sup> D. I. Lersch,<sup>7</sup> H. Li,<sup>3</sup> W. Li,<sup>28</sup> B. Liu,<sup>11</sup> K. Livingston,<sup>9</sup> G. J. Lolos,<sup>23</sup> V. Lyubovitskij,<sup>25,26</sup> D. Mack,<sup>14</sup> H. Marukyan,<sup>27</sup> V. Matveev,<sup>13</sup> M. McCaughan,<sup>14</sup> M. McCracken,<sup>3</sup> W. McGinley,<sup>3</sup> J. McIntyre,<sup>5</sup> C. A. Meyer,<sup>3</sup> R. Miskimen,<sup>15</sup> R. E. Mitchell,<sup>12</sup> F. Mokaya,<sup>5</sup> F. Nerling,<sup>10</sup> L. Ng,<sup>7</sup> A. I. Ostrovidov,<sup>7</sup> Z. Papandreou,<sup>23</sup> M. Patsyuk,<sup>16</sup> P. Pauli,<sup>9</sup> R. Pedroni,<sup>19</sup> L. Pentchev,<sup>14,\*</sup> K. J. Peters,<sup>10</sup> W. Phelps,<sup>8</sup> E. Pooser,<sup>14</sup> N. Qin,<sup>21</sup> J. Reinhold,<sup>6</sup> B. G. Ritchie,<sup>1</sup> L. Robison,<sup>21</sup> D. Romanov,<sup>17</sup> C. Romero,<sup>24</sup> C. Salgado,<sup>18</sup> A. M. Schertz,<sup>28</sup> R. A. Schumacher,<sup>3</sup> J. Schwiening,<sup>10</sup> K. K. Seth,<sup>21</sup> X. Shen,<sup>11</sup> M. R. Shepherd,<sup>12</sup> E. S. Smith,<sup>14</sup> D. I. Sober,<sup>4</sup> A. Somov,<sup>14</sup> S. Somov,<sup>17</sup> O. Soto,<sup>24</sup> J. R. Stevens,<sup>28</sup> I. I. Strakovsky,<sup>8</sup> K. Suresh,<sup>23</sup> V. Tarasov,<sup>13</sup> S. Taylor,<sup>14</sup> A. Teymurazyan,<sup>23</sup> A. Thiel,<sup>9</sup> G. Vasileiadis,<sup>2</sup> D. Werthmüller,<sup>9</sup> T. Whitlatch,<sup>14</sup> N. Wickramaarachchi,<sup>22</sup> M. Williams,<sup>16</sup> T. Xiao,<sup>21</sup> Y. Yang,<sup>16</sup> J. Zarling,<sup>12</sup> Z. Zhang,<sup>29</sup> G. Zhao,<sup>11</sup> Q. Zhou,<sup>11</sup> X. Zhou,<sup>29</sup> and B. Zihlmann<sup>14</sup>

Jlab-Hall D (GlueX Collaboration)



malization, we determine upper limits at 90% confidence level of 4.6%, 2.3%, and 3.8% for  $P_c^+(4312)$ ,  $P_c^+(4440)$ , and  $P_c^+(4457)$ , respectively. These upper limits become a



$$W = s = (q + p_1)^2; t = (p_1 - p_2)^2$$

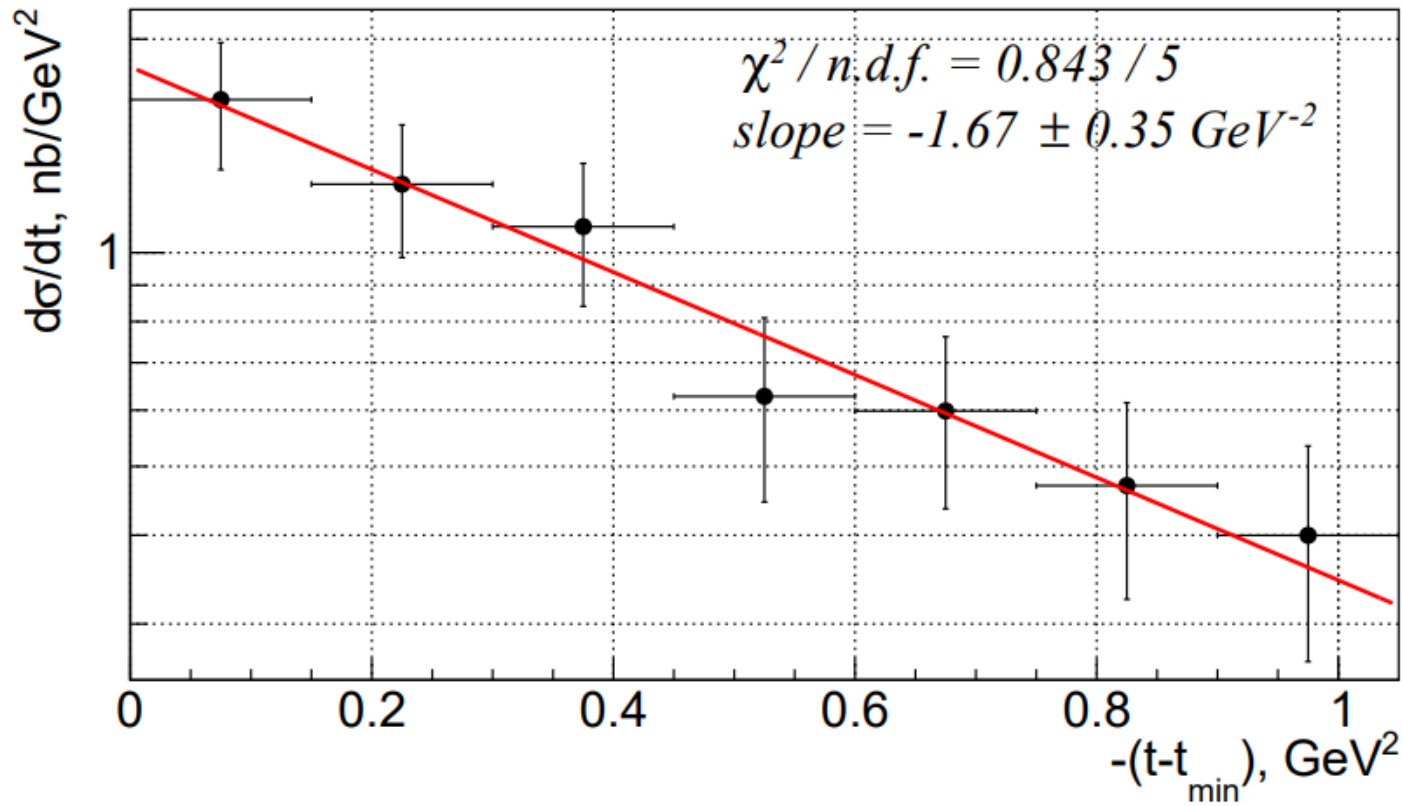


FIG. 3: Differential cross section for  $J/\psi$  photoproduction as a function of  $-(t - t_{\min})$  for  $10.00 < E_\gamma < 11.80$  GeV.




# Mass Radius of Protons

## arXiv:2102.00110

PHYSICAL REVIEW D **104**, 054015 (2021)

---

### Mass radius of the proton

Dmitri E. Kharzeev 

*Center for Nuclear Theory, Department of Physics and Astronomy, Stony Brook University,  
New York 11794-3800, USA*

*and Department of Physics and RIKEN-BNL Research Center, Brookhaven National Laboratory,  
Upton, New York 11973-5000, USA*



(Received 4 February 2021; accepted 20 August 2021; published 15 September 2021)

The mass radius is a fundamental property of the proton that so far has not been determined from experiment. Here, we show that the mass radius of the proton can be rigorously defined through the form factor of the trace of the energy-momentum tensor (EMT) of QCD in the weak gravitational field approximation, as appropriate for this problem. We then demonstrate that the scale anomaly of QCD enables the extraction of the form factor of the trace of the EMT from the data on threshold photoproduction of  $J/\psi$  and  $\Upsilon$  quarkonia, and use the recent GlueX Collaboration data to extract the

# Energy Momentum Tensor $T_{\mu\nu}$

$$\begin{aligned}\langle \mathbf{p}_1 | T_{\mu\nu} | \mathbf{p}_2 \rangle = & \left( \frac{M^2}{p_{01} p_{02}} \right)^{1/2} \frac{1}{4M} \bar{u}(p_1, s_1) \left[ G_1(q^2) (p_\mu \gamma_\nu + p_\nu \gamma_\mu) + G_2(q^2) \frac{p_\mu p_\nu}{M} + \right. \\ & \left. + G_3(q^2) \frac{(q^2 g_{\mu\nu} - q_\mu q_\nu)}{M} \right] u(p_2, s_2),\end{aligned}$$

In the limit of vanishing momentum transfer  $q_\mu \rightarrow 0$ , the forward matrix element of the energy-momentum tensor takes the form,

$$\langle \mathbf{p} | T_{\mu\nu} | \mathbf{p} \rangle = \left( \frac{M^2}{p_0^2} \right)^{1/2} \bar{u}(p, s) u(p, s) \frac{p_\mu p_\nu}{M^2} [G_1(0) + G_2(0)],$$

# Trace of the EMT: $T = T^\mu_\mu$

$$\langle \mathbf{p}_1 | T | \mathbf{p}_2 \rangle = \left( \frac{M^2}{p_{01} p_{02}} \right)^{1/2} \bar{u}(p_1, s_1) u(p_2, s_2) G(q^2), \quad (19)$$

Lorentz-invariant scalar gravitational form factor

$$G(q^2) = G_1(q^2) + G_2(q^2) \left( 1 - \frac{q^2}{4M^2} \right) + G_3(q^2) \frac{3q^2}{4M^2}.$$

Mass radius

$$\langle R_m^2 \rangle = \frac{6}{M} \left. \frac{dG}{dt} \right|_{t=0}$$

In the rest frame of the particle,

$$\langle \mathbf{p} = 0 | T | \mathbf{p} = 0 \rangle = \langle \mathbf{p} = 0 | T_{00} | \mathbf{p} = 0 \rangle = M; \quad (21)$$

therefore,

$$G(0) = M, \quad (22)$$

# Scale (Trace) Anomaly of QCD

In QCD, quantum effects lead to a nonvanishing trace of the EMT even for massless quarks.

$$T \equiv T^\mu_\mu = \frac{\tilde{\beta}(g)}{2g} G^{\mu\nu a} G^a_{\mu\nu} + \sum_{l=u,d,s} m_l (1 + \gamma_{m_l}) \bar{q}_l q_l, \quad (28)$$

In the chiral limit, the information about the mass radius of the proton is contained in the matrix element of the scalar gluon operator in (28) at a nonzero momentum transfer. The zero-momentum transfer, forward matrix element of this operator, yields the proton's mass, and this can be used for evaluating the scattering length in quarkonium-nucleon interaction [7,24,25].

# Measurements of $G(t)$ :

Photoproduction of vector heavy quarkonium states,  $J/\psi$  and  $\Upsilon$  close to the threshold

- (1) Because  $J/\psi$  and  $\Upsilon$  are made of a heavy quark and an antiquark, and the proton at small momentum transfer contains only light quarks, the corresponding amplitude is dominated by the exchange of gluons.
- (2) Close to the threshold, the characteristic size of the heavy quark-antiquark pair is  $\sim 1/(2m_h)$ ; for charm quarks, this is about 0.08 fm. Because this size is much smaller than  $1/\Lambda_{\text{QCD}}$ , the coupling of gluons to the heavy quark is perturbative, is characterized by a small coupling constant, and can be described by a local color-neutral gluon operator of the lowest possible dimension [26–28].

# Measurements of $G(t)$ :

Photoproduction of vector heavy quarkonium states,  $J/\psi$  and  $\Upsilon$  close to the threshold

- (3) Because of the vector quantum numbers  $J^{PC} = 1^{--}$  of  $J/\psi$  and  $\Upsilon$ , the threshold photoproduction is due to the  $t$ —channel exchange of gluons in scalar  $0^{++}$  and tensor  $2^{++}$  states; the scalar exchange is described by the operator that is proportional to the first term in (28). Because of the scale anomaly, its matrix element does not depend on the QCD coupling constant  $g^2$ , whereas the matrix element of the tensor operator appears proportional to  $g^2$  and is subleading at weak coupling [7,8,24,25,29].

# Mass Radius of Protons

Differential cross section  $d\sigma/dt$  is related to  $G(t)$ !

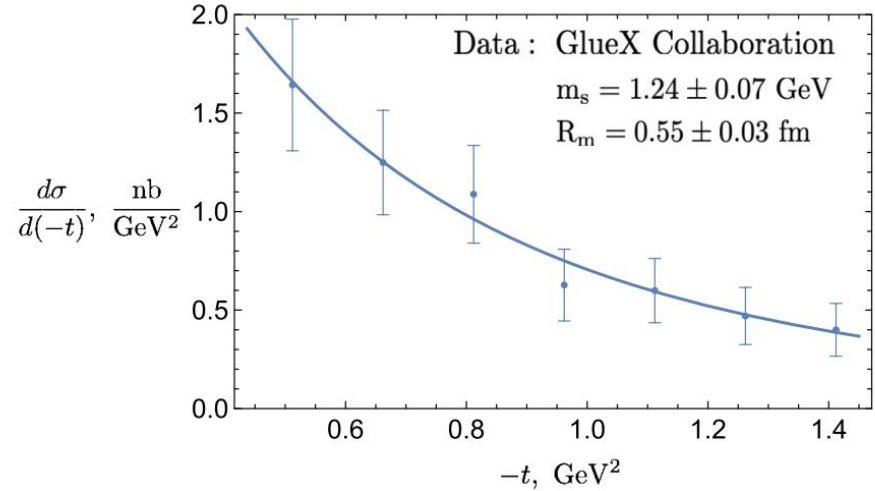
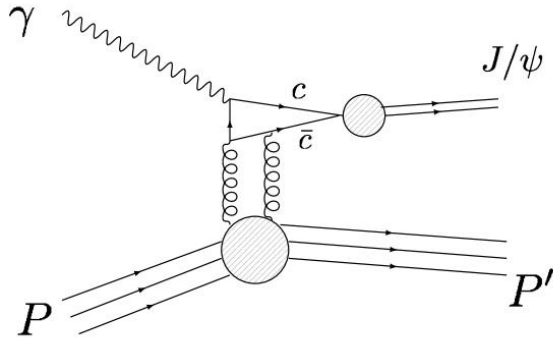


FIG. 1. Left: the Feynman diagram of  $J/\psi$  photoproduction off a proton. Right: the differential cross section of  $J/\psi$  photoproduction at the center-of-mass energy  $E_{cm} = 4.58$  GeV (laboratory energy of the photon  $E_\gamma = 10.72$  GeV, minimum momentum transfer  $t_{min} \simeq -0.44$  GeV<sup>2</sup>); the data is from the GlueX Collaboration [9]. The theory curve corresponds to the dipole form of the scalar gravitational form factor with the parameter  $m_s = 1.24 \pm 0.07$  GeV, corresponding to the mass radius of the proton  $R_m = 0.55 \pm 0.03$  fm.

$$\frac{d\sigma_{\gamma P \rightarrow \psi P}}{dt} = \frac{1}{64\pi s} \frac{1}{|\mathbf{p}_{\gamma cm}|^2} |\mathcal{M}_{\gamma P \rightarrow \psi P}(t)|^2, \quad (34)$$

$$\mathcal{M}_{\gamma P \rightarrow \psi P}(t) = -Qec_2 \frac{16\pi^2 M}{b} \langle P' | T | P \rangle$$

$$\langle \mathbf{p}_1 | T | \mathbf{p}_2 \rangle = \left( \frac{M^2}{p_{01} p_{02}} \right)^{1/2} \bar{u}(p_1, s_1) u(p_2, s_2) G(q^2),$$

$$G(t) = \frac{M}{\left(1 - \frac{t}{m_s^2}\right)^2} \quad \langle R_m^2 \rangle = \frac{12}{m_s^2}$$

$$m_s = 1.24 \pm 0.07 \text{ GeV}$$

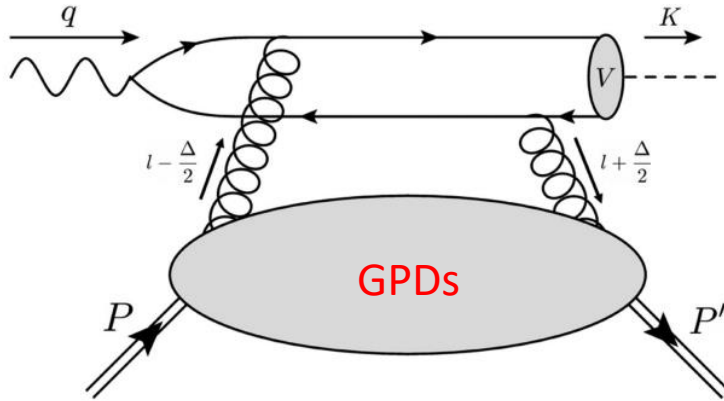
$$R_m \equiv \sqrt{\langle R_m^2 \rangle} = 0.55 \pm 0.03 \text{ fm}$$



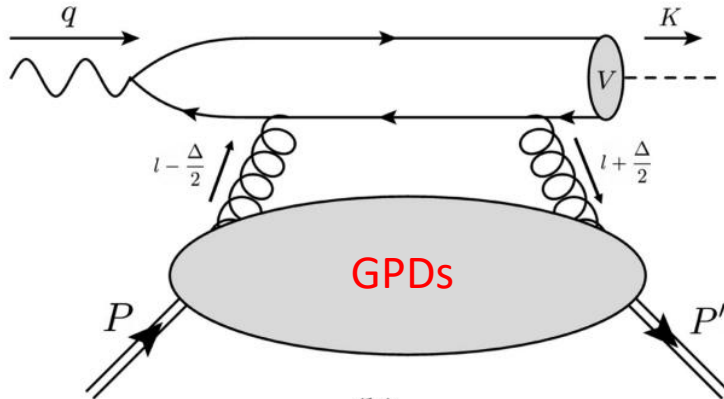
# Photoproduction of $J/\psi$ in GPDs

## Diagrams

(PRD 103, 096010 (2021))



(a)



(b)

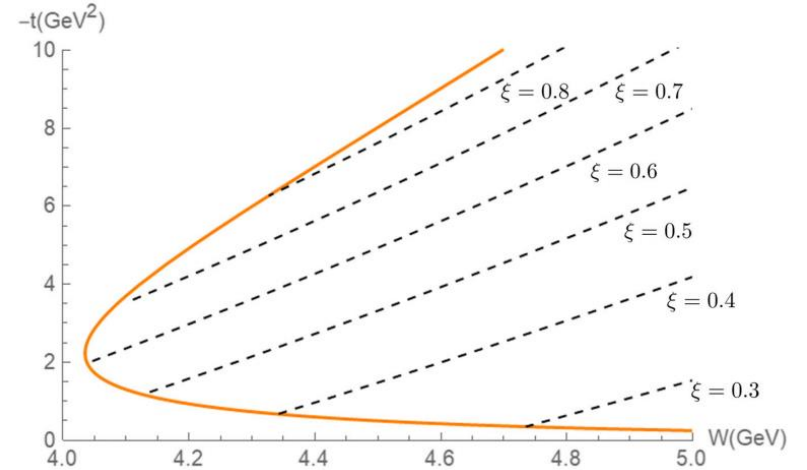


FIG. 2.  $\xi$  on the  $(W, -t)$  plane in the kinematically allowed region with  $M_{J/\psi} = 3.097$  GeV.

$$\begin{aligned} \frac{d\sigma}{dt} &= \frac{e^2 e_Q^2}{16\pi(W^2 - M_N^2)^2} \frac{1}{2} \sum_{\text{polarization}} |\mathcal{M}(\varepsilon_V, \varepsilon)|^2, \\ &= \frac{\alpha_{\text{EM}} e_Q^2}{4(W^2 - M_N^2)^2} \frac{(16\pi\alpha_S)^2}{3M_V^3} |\psi_{\text{NR}}(0)|^2 |G(t, \xi)|^2, \end{aligned} \quad (17)$$

**Gluon GPDs**

Differential cross section  $d\sigma/dt$  is related to gluon GPDs!



# A, B and C Form Factors

$$|G(t, \xi)|^2 = \frac{1}{\xi^4} \left\{ \left( 1 - \frac{t}{4M_N^2} \right) E_2^2 - 2E_2(H_2 + E_2) + (1 - \xi^2)(H_2 + E_2)^2 \right\},$$

$$\int_0^1 dx H_g(x, \xi, t) = \boxed{A_{2,0}^g(t)} + (2\xi)^2 \boxed{C_2^g} \equiv H_2(t, \xi),$$

$$\int_0^1 dx E_g(x, \xi, t) = \boxed{B_{2,0}^g(t)} - (2\xi)^2 \boxed{C_2^g} \equiv E_2(t, \xi).$$

The cross section of heavy vector-meson photoproduction can be expressed in terms of the (gravitational) form factors,  $A_2$ ,  $B_2$  and  $C_2$ .

# A, B and C Form Factors and $T_{\mu\nu}$

$$\begin{aligned} \langle P' | T_{q,g}^{\mu\nu} | P \rangle = & \bar{u}(P') \left[ A_{q,g}(t) \gamma^{(\mu} \bar{P}^{\nu)} + B_{q,g}(t) \frac{\bar{P}^{(\mu} i \sigma^{\nu)\alpha} \Delta_\alpha}{2M_N} \right. \\ & \left. + C_{q,g}(t) \frac{\Delta^\mu \Delta^\nu - g^{\mu\nu} \Delta^2}{M_N} + \bar{C}_{q,g}(t) M_N g^{\mu\nu} \right] u(P), \end{aligned} \quad (25)$$

where  $A = A_{2,0}$ ,  $B = B_{2,0}$ , and  $C = C_{2,0}$  are the same form factors as in Eq. (23). It leads to the following form of

$$\int_0^1 dx H_g(x, \xi, t) = A_{2,0}^g(t) + (2\xi)^2 C_2^g \equiv H_2(t, \xi),$$

$$\int_0^1 dx E_g(x, \xi, t) = B_{2,0}^g(t) - (2\xi)^2 C_2^g \equiv E_2(t, \xi).$$

# Extraction of A and C

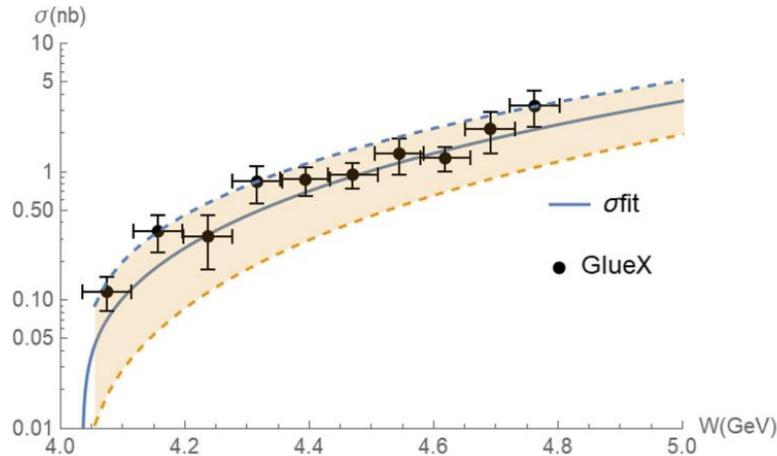


FIG. 6. Fit total cross section for  $J/\psi$  production compared with the total cross section measured at GlueX [36]. The 95% confidence band is shown as the shaded region hereafter.

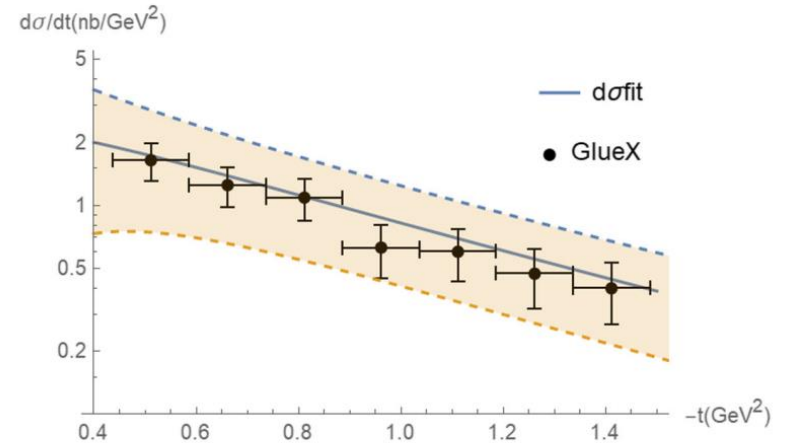


FIG. 7. Fit differential cross section for  $J/\psi$  production compared with the differential cross section at  $W = 4.58$  GeV measured at GlueX [36].

$$A_g(t) = \frac{A_g(0)}{\left(1 - \frac{t}{m_A^2}\right)^2}$$

$$C_g(t) = \frac{C_g(0)}{\left(1 - \frac{t}{m_C^2}\right)^2}$$

# Scalar and Mass Radius

The scalar and mass radii of the proton are defined as [34]

$$\begin{aligned}\langle r^2 \rangle_s &= 6 \frac{dA(t)}{dt} - 18 \frac{C(0)}{M_N^2}, \\ \langle r^2 \rangle_m &= 6 \frac{dA(t)}{dt} - 6 \frac{C(0)}{M_N^2}.\end{aligned}\tag{43}$$

$$\langle r^2 \rangle_A \equiv 6 \frac{dA(t)}{dt} \approx (0.42 \text{ fm})^2,\tag{46}$$

$$\langle r^2 \rangle_C \equiv -6 \frac{C(0)}{M_N^2} \approx (0.54 \text{ fm})^2,\tag{47}$$

and then we have

$$\langle r^2 \rangle_s \approx (1.03 \text{ fm})^2,\tag{48}$$

$$\langle r^2 \rangle_m \approx (0.68 \text{ fm})^2.\tag{49}$$

# Scalar Radius of the Proton

The **scalar radius of the proton** refers to the spatial distribution of the scalar quark density inside the proton, usually defined via the slope of the scalar form factor at zero momentum transfer. It is different from the more familiar **charge radius** (from the electromagnetic form factor) or the **axial radius** (from the axial form factor).

Formally, the scalar radius is defined through the scalar form factor  $F_S(Q^2)$ :

$$\langle p' | \bar{q}q | p \rangle = \bar{u}(p') u(p) F_S(Q^2),$$

and the **scalar radius** is extracted as

$$\langle r_S^2 \rangle = -\frac{6}{F_S(0)} \left. \frac{dF_S(Q^2)}{dQ^2} \right|_{Q^2=0}.$$

# “007”: Nature 615 (2023) 7954, 813 arXiv:2207.05212

## Article

# Determining the gluonic gravitational form factors of the proton

<https://doi.org/10.1038/s41586-023-05730-4>

Received: 8 June 2022

Accepted: 13 January 2023

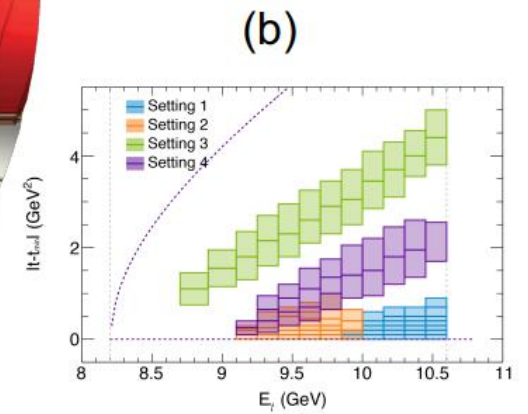
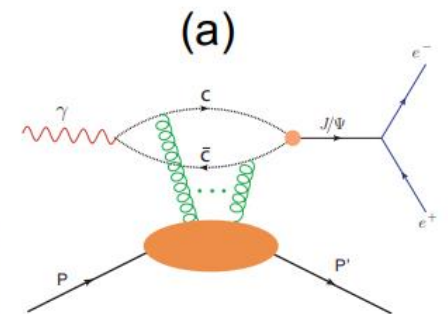
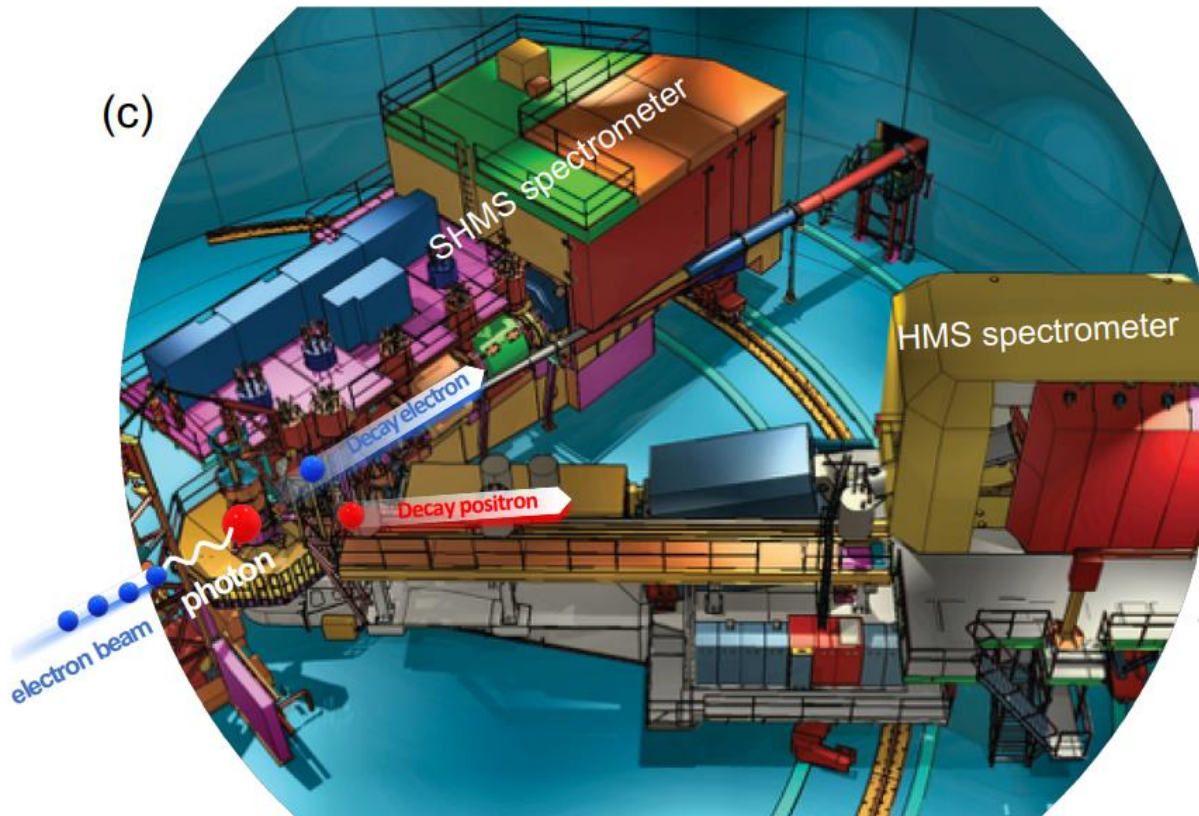
Published online: 29 March 2023



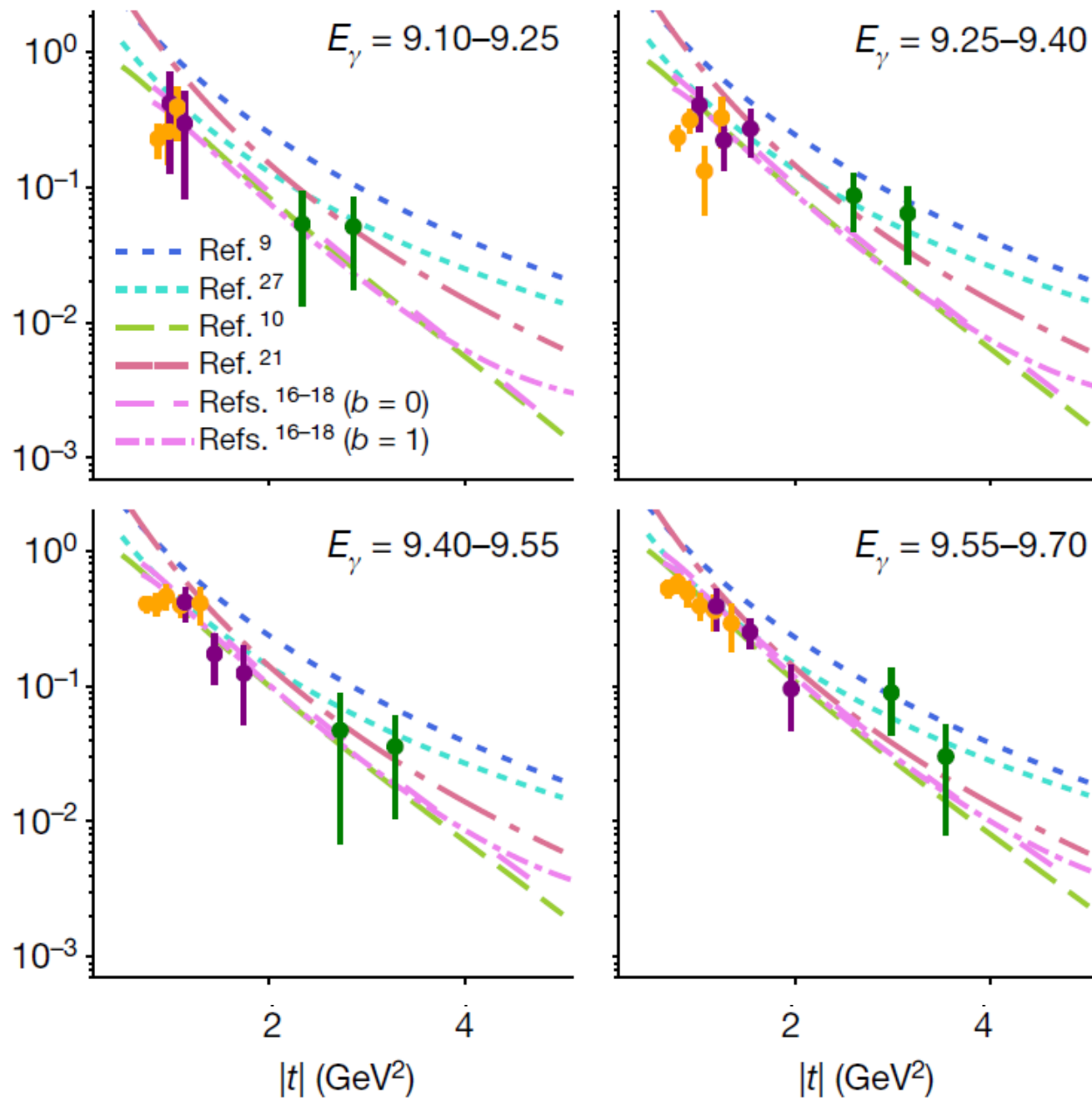
Check for updates

B. Duran<sup>1,2</sup>, Z.-E. Meziani<sup>1,2</sup>✉, S. Joosten<sup>1</sup>, M. K. Jones<sup>3</sup>, S. Prasad<sup>1</sup>, C. Peng<sup>1</sup>, W. Armstrong<sup>1</sup>, H. Atac<sup>2</sup>, E. Chudakov<sup>3</sup>, H. Bhatt<sup>4</sup>, D. Bhetuwal<sup>4</sup>, M. Boer<sup>5</sup>, A. Camsonne<sup>3</sup>, J.-P. Chen<sup>3</sup>, M. M. Dalton<sup>3</sup>, N. Deokar<sup>2</sup>, M. Diefenthaler<sup>3</sup>, J. Dunne<sup>4</sup>, L. El Fassi<sup>4</sup>, E. Fuchey<sup>6</sup>, H. Gao<sup>7</sup>, D. Gaskell<sup>3</sup>, O. Hansen<sup>3</sup>, F. Hauenstein<sup>8</sup>, D. Higinbotham<sup>3</sup>, S. Jia<sup>2</sup>, A. Karki<sup>4</sup>, C. Keppel<sup>3</sup>, P. King<sup>9</sup>, H. S. Ko<sup>10</sup>, X. Li<sup>7</sup>, R. Li<sup>2</sup>, D. Mack<sup>3</sup>, S. Malace<sup>3</sup>, M. McCaughan<sup>3</sup>, R. E. McClellan<sup>11</sup>, R. Michaels<sup>3</sup>, D. Meekins<sup>3</sup>, Michael Paolone<sup>2</sup>, L. Pentchev<sup>3</sup>, E. Pooser<sup>3</sup>, A. Puckett<sup>6</sup>, R. Radloff<sup>9</sup>, M. Rehfuss<sup>2</sup>, P. E. Reimer<sup>1</sup>, S. Riordan<sup>1</sup>, B. Sawatzky<sup>3</sup>, A. Smith<sup>7</sup>, N. Sparveris<sup>2</sup>, H. Szumila-Vance<sup>3</sup>, S. Wood<sup>3</sup>, J. Xie<sup>1</sup>, Z. Ye<sup>1</sup>, C. Yero<sup>8</sup> & Z. Zhao<sup>7</sup>

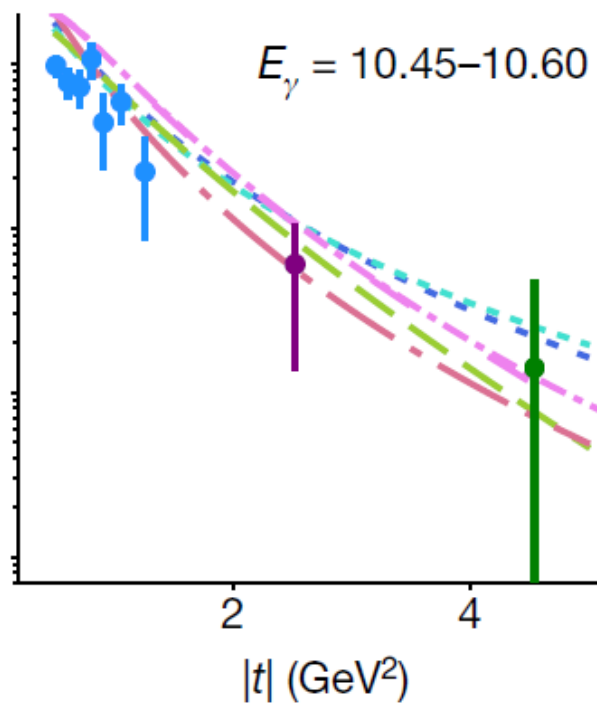
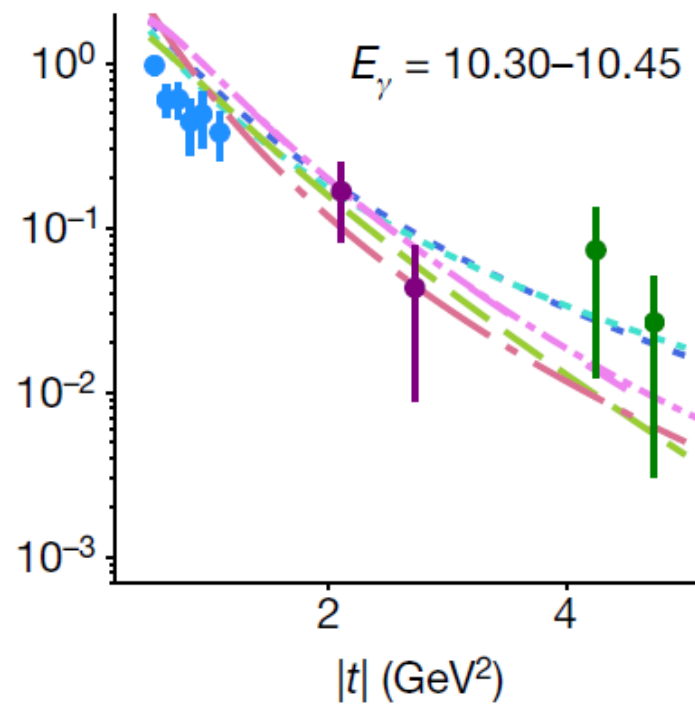
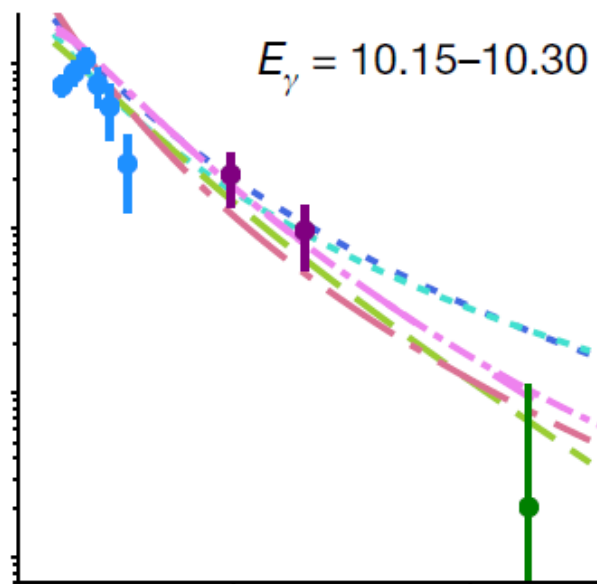
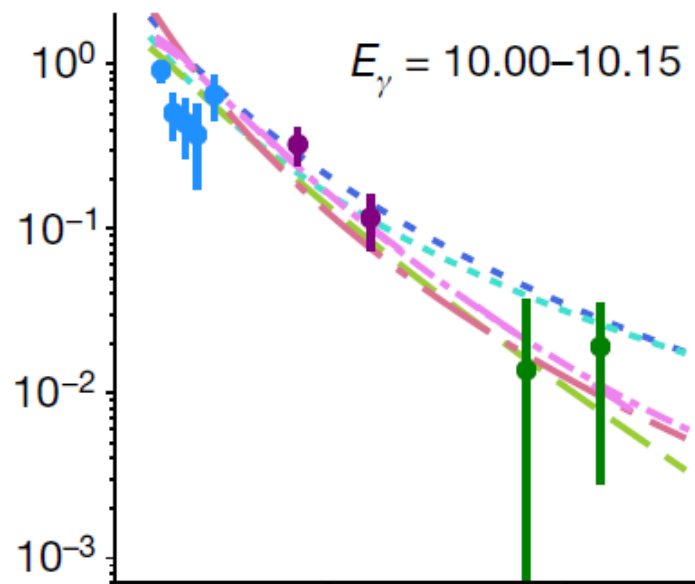
The proton is one of the main building blocks of all visible matter in the Universe<sup>1</sup>. Among its intrinsic properties are its electric charge, mass and spin<sup>2</sup>. These properties emerge from the complex dynamics of its fundamental constituents—quarks and



Jlab-Hall C







$$\langle r_m^2 \rangle_g = 6 \frac{1}{A_g(0)} \frac{dA_g(t)}{dt} \Big|_{t=0} - 6 \frac{1}{A_g(0)} \frac{C_g(0)}{M_N^2}$$

$$\langle r_s^2 \rangle_g = 6 \frac{1}{A_g(0)} \frac{dA_g(t)}{dt} \Big|_{t=0} - 18 \frac{1}{A_g(0)} \frac{C_g(0)}{M_N^2}$$








**Table 1.** Gluonic GFF parameters and corresponding proton mass and scalar radii, determined from our data through a two-dimensional fit following the holographic QCD and the GPD+VMD approach, compared to the latest lattice results<sup>9</sup>. In all cases we used the tripole-tripole functional form approximation for the GFFs. Note the similar  $\chi^2/\text{ndf}$  in both cases.

Theoretical approach GFF functional form	$\chi^2/\text{n.d.f}$	$m_A$ (GeV <sup>2</sup> )	$m_C$ (GeV <sup>2</sup> )	$C_g(0)$	$\sqrt{\langle r_m^2 \rangle}$ (fm)	$\sqrt{\langle r_s^2 \rangle}$ (fm)
Holographic QCD Tripole-tripole	0.925	$1.575 \pm 0.059$	$1.12 \pm 0.21$	$-0.45 \pm 0.132$	$0.755 \pm 0.035$	$1.069 \pm 0.056$
GPD + VMD Tripole-tripole	0.924	$2.71 \pm 0.19$	$1.28 \pm 0.50$	$-0.20 \pm 0.11$	$0.472 \pm 0.042$	$0.695 \pm 0.071$
Lattice Tripole-tripole		$1.641 \pm 0.043$	$1.07 \pm 0.12$	$-0.483 \pm 0.133$	$0.7464 \pm 0.025$	$1.073 \pm 0.066$

# Eur. Phys. J. C (2020) 80:1053

<https://doi.org/10.1140/epjc/s10052-020-08620-5>

## Deciphering the mechanism of near-threshold $J/\psi$ photoproduction

Meng-Lin Du<sup>1</sup>, Vadim Baru<sup>1,2,3</sup>, Feng-Kun Guo<sup>4,5,a</sup>, Christoph Hanhart<sup>6</sup>, Ulf-G. Meißner<sup>1,6,7</sup>, Alexey Nefediev<sup>3,8,9</sup>, Igor Strakovsky<sup>10</sup>

<sup>1</sup> Helmholtz-Institut für Strahlen- und Kernphysik and Bethe Center for Theoretical Physics, Universität Bonn, 53115 Bonn, Germany

<sup>2</sup> Institute for Theoretical and Experimental Physics NRC “Kurchatov Institute”, Moscow 117218, Russia

<sup>3</sup> P.N. Lebedev Physical Institute of the Russian Academy of Sciences, Leninskiy Prospect 53, Moscow 119991, Russia

<sup>4</sup> CAS Key Laboratory of Theoretical Physics, Institute of Theoretical Physics, Chinese Academy of Sciences, Zhong Guan Cun East Street 55, Beijing 100190, China

<sup>5</sup> School of Physical Sciences, University of Chinese Academy of Sciences, Beijing 100049, China

<sup>6</sup> Institute for Advanced Simulation, Institut für Kernphysik and Jülich Center for Hadron Physics, Forschungszentrum Jülich, 52425 Jülich, Germany

<sup>7</sup> Tbilisi State University, 0186 Tbilisi, Georgia

<sup>8</sup> Moscow Institute of Physics and Technology, Institutsky lane 9, Dolgoprudny, Moscow Region 141700, Russia

<sup>9</sup> National Research Nuclear University MEPhI, Kashirskoe highway 31, Moscow 115409, Russia

<sup>10</sup> Department of Physics, Institute for Nuclear Studies, The George Washington University, Washington, DC 20052, USA

Received: 11 October 2020 / Accepted: 30 October 2020 / Published online: 16 November 2020

© The Author(s) 2020

# Coupled-channel Mechanism & Hadronic Interactions

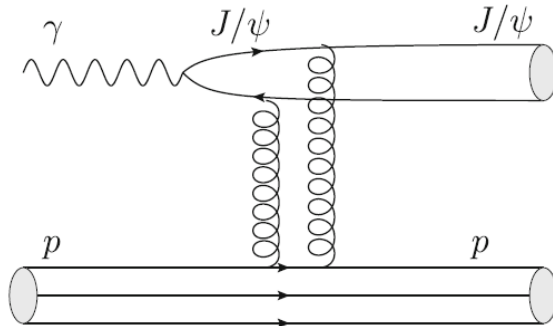


**Fig. 1** Vector-meson dominance model mechanism for the near-threshold  $J/\psi$  photoproduction

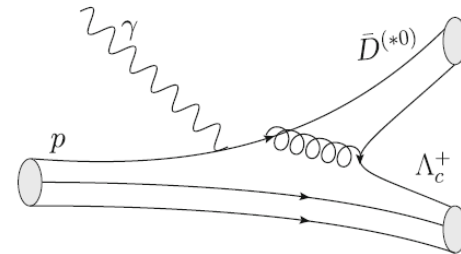


**Fig. 2** Mechanism for the near-threshold  $J/\psi$  photoproduction through  $\Lambda_c \bar{D}^{(*)}$  which then rescatter into  $J/\psi p$

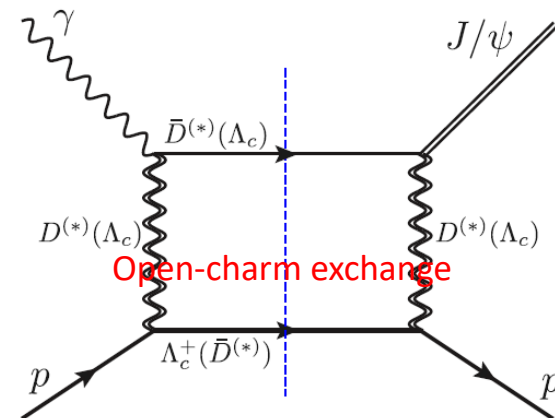


**Fig. 3** Feynman diagram for the proposed CC mechanism. The dashed blue line pinpoints the open-charm intermediate state

# Threshold cusps

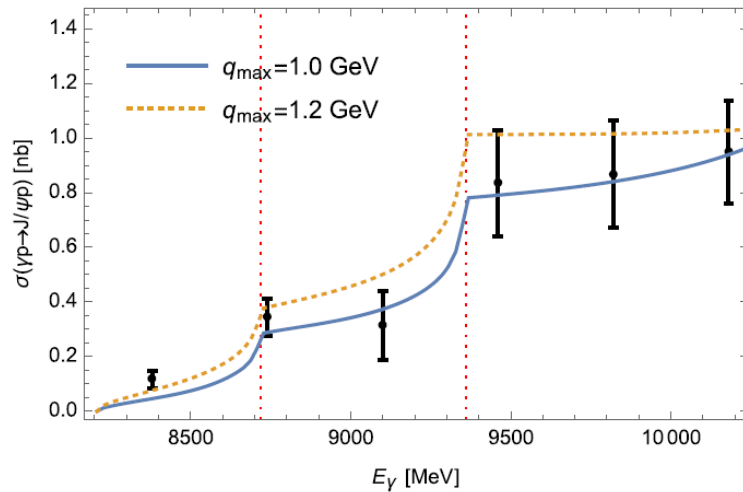


**Fig. 4** Comparison of the  $J/\psi$  photoproduction through the open-charm loops as shown in Figs. 2 and 3 with the GlueX data [19].  $E_\gamma$  is the photon energy in the rest frame of the initial proton. Since we consider only the  $\Lambda_c \bar{D}^{(*)}$  channels, the comparison with the data is only shown up to  $E_\gamma = 10.2$  GeV though a qualitative agreement up to the highest GlueX data point 11.6 GeV is also achieved. The vertical dotted lines indicate the  $\Lambda_c \bar{D}^{(*)}$  thresholds

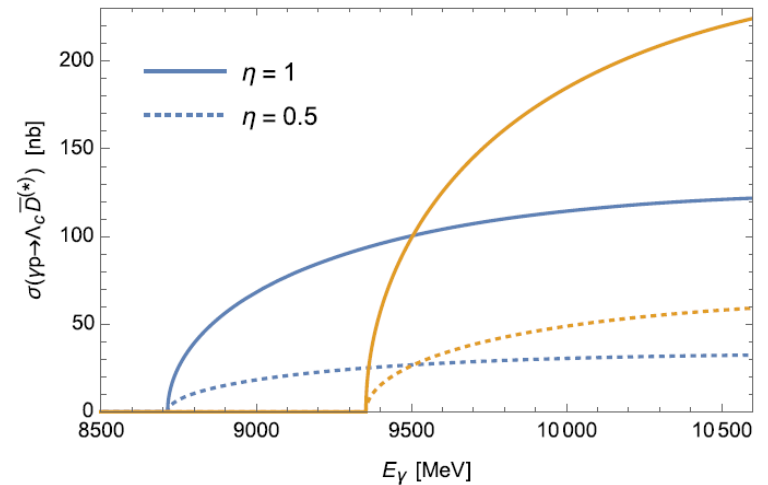


**Fig. 5** Estimates of the cross sections for the  $\gamma p \rightarrow \Lambda_c \bar{D}^{(*)}$  (blue curves) and  $\gamma p \rightarrow \Lambda_c \bar{D}^{(*)}$  (orange curves) reactions

The cross sections of the  $\gamma p \rightarrow \Lambda_c \bar{D}^{(*)}$  reactions were calculated in Ref. [30] considering exchanges of  $s$ -channel hidden-charm pentaquarks and  $t$ -channel  $D^*$  mesons using the VMD model. The corresponding predictions appear an

# GlueX: PRC 108, 025201 (2023)

PHYSICAL REVIEW C **108**, 025201 (2023)

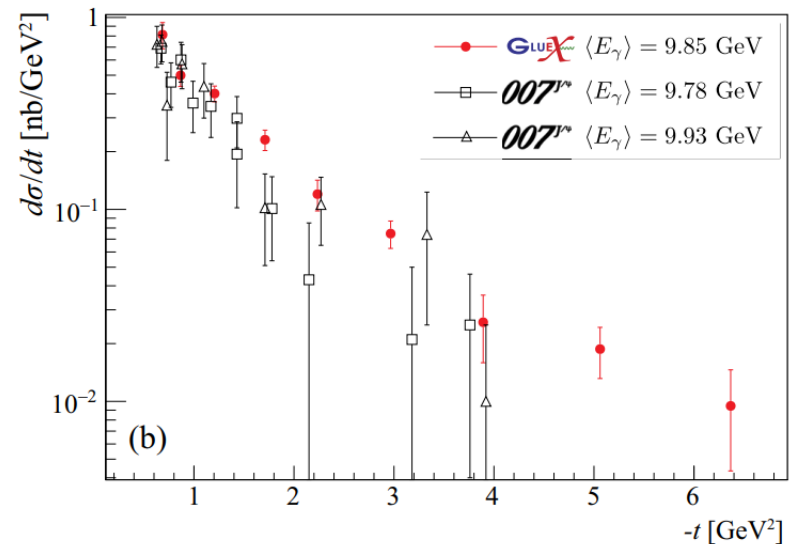
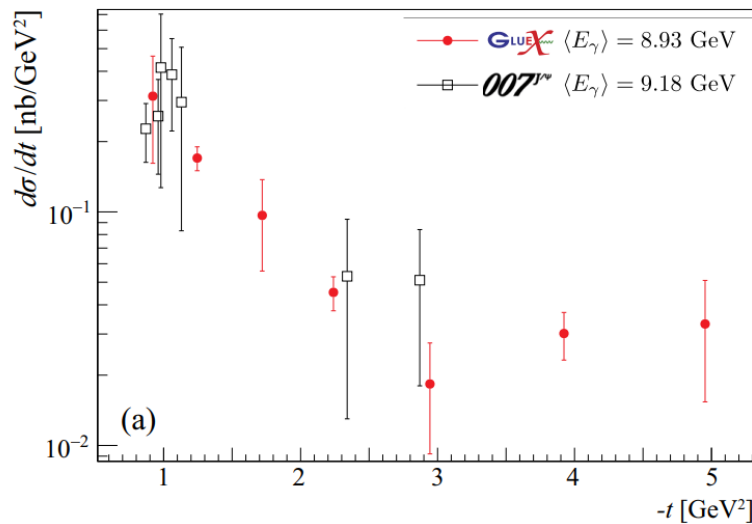
Editors' Suggestion

## Measurement of the $J/\psi$ photoproduction cross section over the full near-threshold kinematic region

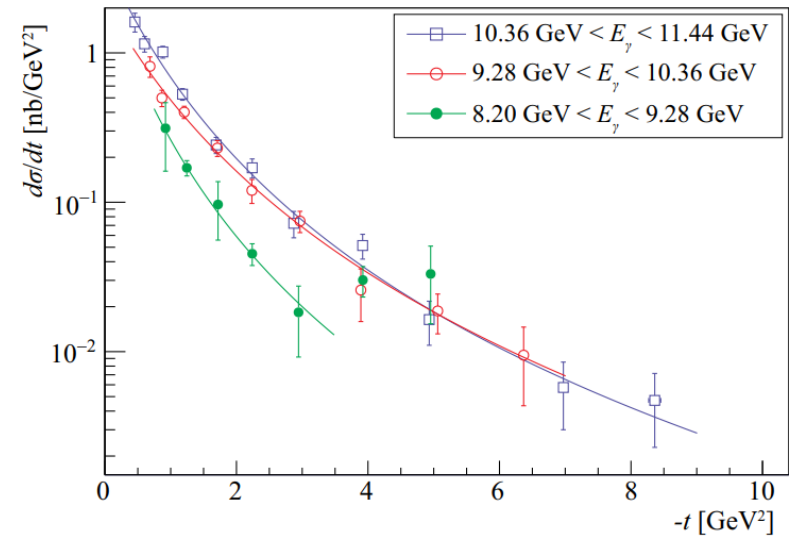
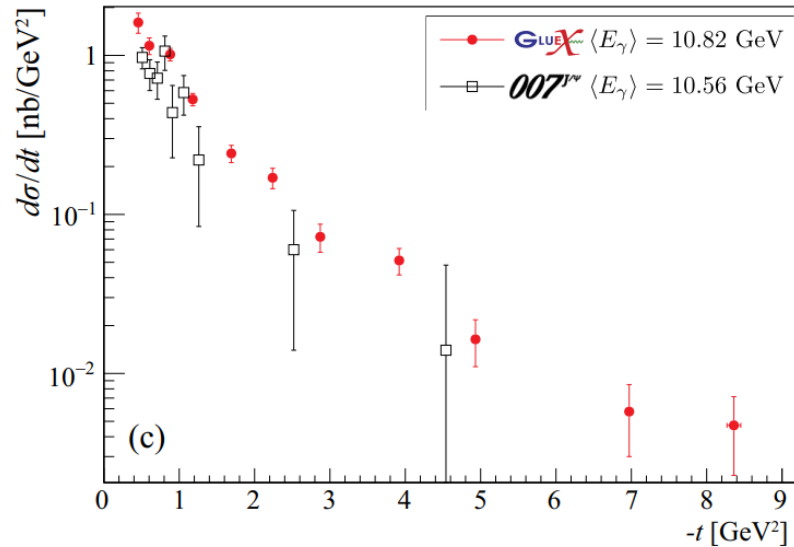
S. Adhikari,<sup>26</sup> F. Afzal,<sup>3</sup> C. S. Akondi,<sup>9</sup> M. Albrecht,<sup>29</sup> M. Amarian,<sup>26</sup> V. Arroyave,<sup>8</sup> A. Asaturyan,<sup>25,36</sup> A. Austregesilo,<sup>29</sup> Z. Baldwin,<sup>4</sup> F. Barbosa,<sup>29</sup> J. Barlow,<sup>9</sup> E. Barriga,<sup>9</sup> R. Barsotti,<sup>14</sup> T. D. Beattie,<sup>27</sup> V. V. Berdnikov,<sup>5</sup> T. Black,<sup>25</sup> W. Boeglin,<sup>8</sup> W. J. Briscoe,<sup>10</sup> T. Britton,<sup>29</sup> W. K. Brooks,<sup>28</sup> D. Byer,<sup>7</sup> E. Chudakov,<sup>29</sup> P. L. Cole,<sup>17</sup> O. Cortes,<sup>10</sup> V. Crede,<sup>9</sup> M. M. Dalton,<sup>29</sup> D. Darulis,<sup>11</sup> A. Deur,<sup>29</sup> S. Dobbs,<sup>9</sup> A. Dolgolenko,<sup>16</sup> R. Dotel,<sup>8</sup> M. Dugger,<sup>1</sup> R. Dzhygadlo,<sup>12</sup> D. Ebersole,<sup>9</sup> H. Egiyan,<sup>29</sup> T. Erbora,<sup>8</sup> P. Eugenio,<sup>9</sup> A. Fabrizi,<sup>19</sup> C. Fanelli,<sup>34</sup> S. Fang,<sup>13</sup> S. Fegan,<sup>10</sup> J. Fitches,<sup>11</sup> A. M. Foda,<sup>12</sup> S. Furlotov,<sup>29</sup> L. Gan,<sup>25</sup> H. Gao,<sup>7</sup> A. Gardner,<sup>1</sup> A. Gasparian,<sup>24</sup> C. Gleason,<sup>14,32</sup> K. Goetzen,<sup>12</sup> V. S. Goryachev,<sup>16</sup> B. Grube,<sup>29</sup> J. Guo,<sup>4</sup> L. Guo,<sup>8</sup> T. J. Hague,<sup>24</sup> H. Hakobyan,<sup>28</sup> J. Hernandez,<sup>9</sup> N. D. Hoffman,<sup>4</sup> D. Hornidge,<sup>22</sup> G. Hou,<sup>13</sup> G. M. Huber,<sup>27</sup> P. Hurck,<sup>11</sup> A. Hurley,<sup>34</sup> W. Imoehl,<sup>4</sup> D. G. Ireland,<sup>11</sup> M. M. Ito,<sup>9</sup> I. Jaegle,<sup>29</sup> N. S. Jarvis,<sup>4</sup> T. Jeske,<sup>29</sup> R. T. Jones,<sup>6</sup> V. Kakoyan,<sup>36</sup> G. Kalicy,<sup>5</sup> V. Khachatryan,<sup>14</sup> M. Khachatryan,<sup>8</sup> C. Kourkoulis,<sup>2</sup> A. LaDuke,<sup>4</sup> I. Larin,<sup>19,16</sup> D. Lawrence,<sup>29</sup> D. I. Lersch,<sup>29</sup> H. Li,<sup>4</sup> W. B. Li,<sup>34</sup> B. Liu,<sup>13</sup> K. Livingston,<sup>11</sup> G. J. Lolos,<sup>27</sup> L. Lorenti,<sup>34</sup> V. Lyubovitskij,<sup>31,30</sup> D. Mack,<sup>29</sup> A. Mahmood,<sup>27</sup> P. P. Martel,<sup>22,18</sup> H. Marukyan,<sup>36</sup> V. Matveev,<sup>16</sup> M. McCaughan,<sup>29</sup> M. McCracken,<sup>4,33</sup> C. A. Meyer,<sup>4</sup> R. Miskimen,<sup>19</sup> R. E. Mitchell,<sup>14</sup> K. Mizutani,<sup>29</sup> V. Neelamana,<sup>27</sup> L. Ng,<sup>9</sup> E. Nissen,<sup>29</sup> S. Orešić,<sup>27</sup> A. I. Ostrovidov,<sup>9</sup> Z. Papandreou,<sup>27</sup> C. Paudel,<sup>8</sup> R. Pedroni,<sup>24</sup> L. Pentchev,<sup>29,\*</sup> K. J. Peters,<sup>12</sup> E. Prather,<sup>6</sup> S. Rakshit,<sup>9</sup> J. Reinhold,<sup>8</sup> A. Remington,<sup>9</sup> B. G. Ritchie,<sup>1</sup> J. Ritman,<sup>12,15</sup> G. Rodriguez,<sup>9</sup> D. Romanov,<sup>21</sup> K. Saldana,<sup>14</sup> C. Salgado,<sup>23</sup> S. Schadmmand,<sup>12</sup> A. M. Schertz,<sup>14</sup> K. Scheuer,<sup>34</sup> A. Schick,<sup>19</sup> A. Schmidt,<sup>10</sup> R. A. Schumacher,<sup>4</sup> J. Schwiening,<sup>12</sup> P. Sharp,<sup>10</sup> X. Shen,<sup>13</sup> M. R. Shepherd,<sup>14</sup> A. Smith,<sup>7</sup> E. S. Smith,<sup>34</sup> D. I. Sober,<sup>5</sup> S. Somov,<sup>21</sup> A. Somov,<sup>29</sup> J. R. Stevens,<sup>34</sup> I. I. Strakovsky,<sup>10</sup> B. Sumner,<sup>1</sup> K. Suresh,<sup>27</sup> V. V. Tarasov,<sup>16</sup> S. Taylor,<sup>29</sup> A. Teymurazyan,<sup>27</sup> A. Thiel,<sup>3</sup> T. Viducic,<sup>26</sup> T. Whitlatch,<sup>29</sup> N. Wickramaarachchi,<sup>5</sup> M. Williams,<sup>20</sup> Y. Wunderlich,<sup>3</sup> B. Yu,<sup>7</sup> J. Zarling,<sup>35</sup> Z. Zhang,<sup>35</sup> Z. Zhao,<sup>7</sup> X. Zhou,<sup>35</sup> J. Zhou,<sup>7</sup> and B. Zihlmann<sup>29</sup>

(GLUEX Collaboration)

# Differential Cross Sections

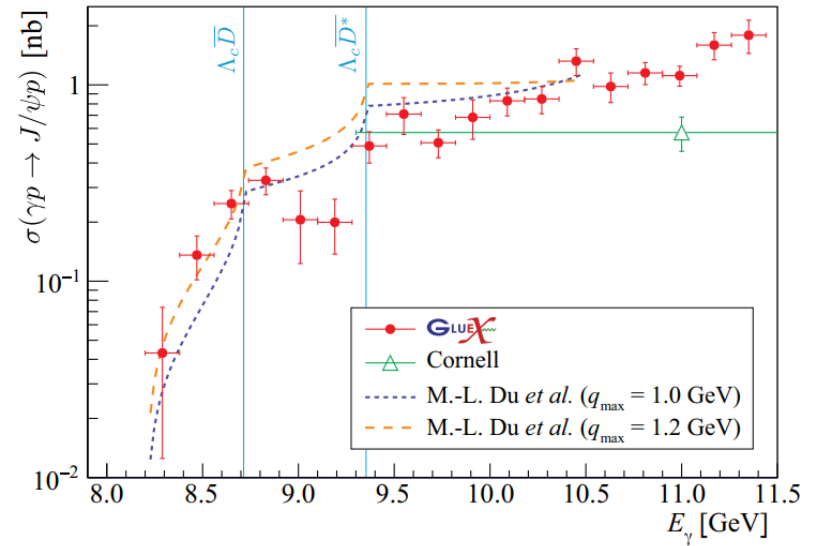
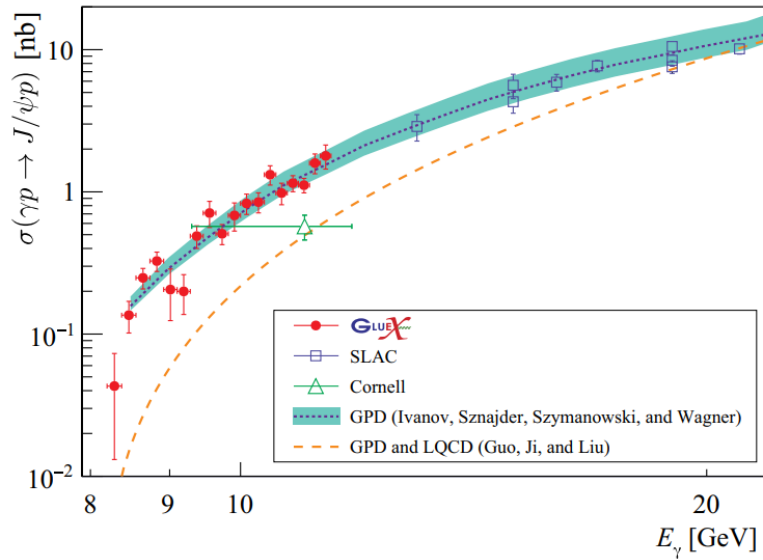


# Differential Cross Sections





# Total Cross Sections



We can use the mass scale  $m_s$  from the fits in Fig. 15 (Table II) to estimate the proton mass radius as prescribed in Ref. [11],

$$\sqrt{\langle r_m^2 \rangle} = \sqrt{\frac{6}{m_p} \left. \frac{dG(t)}{dt} \right|_{t=0}} = \sqrt{\frac{12}{m_s^2}}, \quad (7)$$

where the scalar gravitational form factor,  $G(t)$ , is related to the measured  $t$  distributions through the VMD model. Equation (7) gives  $\sqrt{\langle r_m^2 \rangle} = 0.619 \pm 0.094$  fm,  $0.464 \pm 0.024$  fm, and  $0.521 \pm 0.020$  fm for  $E_\gamma = 8.93, 9.86$ , and  $10.82$  GeV, respectively. More sophisticated estimations of the proton mass radius require knowledge of the  $A(t)$  and  $C(t)$  gravitational form factors separately [10,41].

The authors of Ref. [19] propose an alternative mechanism of  $J/\psi$  photoproduction with a dominant exchange of open-charm channels  $\Lambda_c \bar{D}$  and  $\Lambda_c \bar{D}^*$  in box diagrams. We show the total cross section results of this model in Fig. 18, and find good qualitative agreement with our measurements. In particular, in the data we see structures peaking at both the  $\Lambda_c \bar{D}$  and  $\Lambda_c \bar{D}^*$  thresholds that can be interpreted as the cusps expected with this reaction mechanism. However, the exchange of heavy hadrons in this model implies a very shallow  $t$  dependence in the differential cross sections. This is not supported by the steeply falling cross sections we observe, as shown in Fig. 15. Therefore, our differential cross section measurements do not support a dominant contribution from these open charm exchanges, although the enhancement at high  $t$

proton gluonic form factors. Based on the  $t$ -slopes of the differential cross sections (Fig. 15) and also the results of Ref. [41], the differential cross section at low  $t$  values is consistent with being dominantly due to gluonic exchange. However, the possible structures in the total cross section energy dependence and the flattening of the differential cross section near threshold are consistent with contributions from open-charm intermediate states. So far, from the analyses of Ref. [52] it is not possible to distinguish between the gluon and open-charm exchange mechanisms. Certainly, fur-

# PLB 856, 138904 (2024)

<https://www.sciencedirect.com/science/article/pii/S0370269324004623>

Phys. Lett. B 856 (2024) 138904



Contents lists available at [ScienceDirect](https://www.sciencedirect.com)





Physics Letters B

journal homepage: [www.elsevier.com/locate/physletb](http://www.elsevier.com/locate/physletb)



Letter

## $J/\psi$ photoproduction: Threshold to very high energy

Lin Tang (唐淋)<sup>a,b, </sup>, Yi-Xuan Yang (杨逸轩)<sup>a,b, </sup>, Zhu-Fang Cui (崔著飏)<sup>a,b, </sup>,  
Craig D. Roberts<sup>a,b, </sup>,\*

<sup>a</sup> School of Physics, Nanjing University, Nanjing, Jiangsu 210093, China

<sup>b</sup> Institute for Nonperturbative Physics, Nanjing University, Nanjing, Jiangsu 210093, China



### ARTICLE INFO

Editor: A. Ringwald

#### Keywords:

Continuum Schwinger function methods  
Emergence of mass  
Gluons  
Heavy mesons  
Pomeron  
Proton structure

### ABSTRACT

A reaction model for  $\gamma + p \rightarrow J/\psi + p$  photoproduction, which exposes the  $c\bar{c}$  content of the photon in making the transition  $\gamma \rightarrow c\bar{c} + \mathbb{P} \rightarrow J/\psi$  and couples the intermediate  $c\bar{c}$  system to the proton's valence quarks via Pomeron ( $\mathbb{P}$ ) exchange, is used to deliver a description of available data, viz. both differential and total cross sections from near threshold, where data has newly been acquired, to invariant mass  $W \approx 300$  GeV. The study suggests that it is premature to link existing  $\gamma + p \rightarrow J/\psi + p$  data with, for instance, in-proton gluon distributions, the quantum chromodynamics trace anomaly, or pentaquark production. Further developments in reaction theory and higher precision data are necessary before the validity of any such connections can be assessed.

# Model of Pomeron Exchange

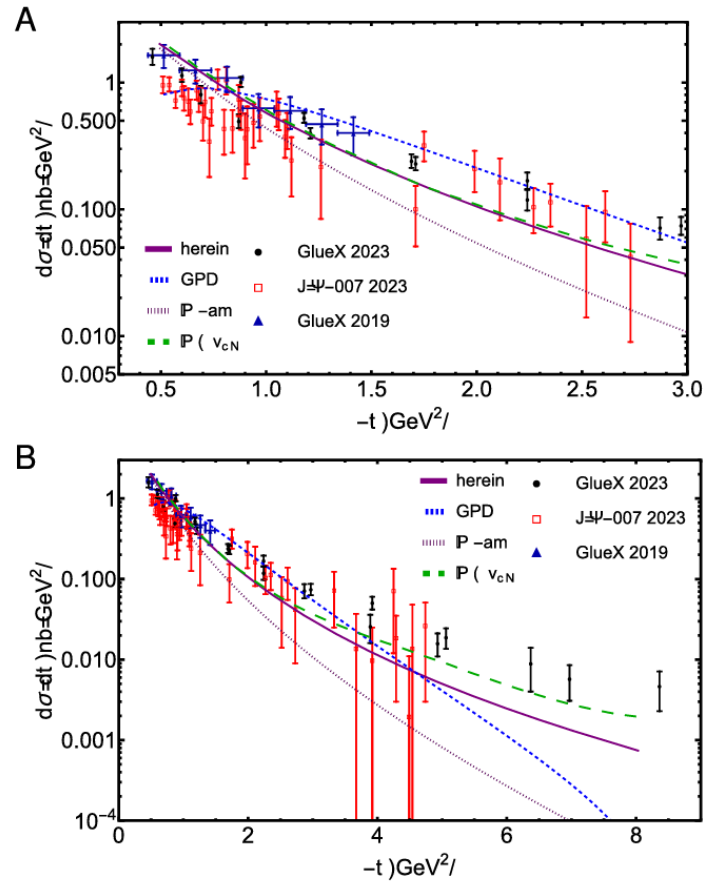


**Table 3**

$\chi^2/\text{dof}$  for each curve drawn in the panels of Fig. 4 – herein, Ref. [19, GPD], Ref. [21,  $\mathbb{P} + v_{cN}$ ], and  $\mathbb{P}$ -am., computed in comparison with various combinations of available near-threshold data [22,23, GlueX], [24,  $J/\psi$ -007]. *N.B.* The GPD model parameters were fitted to obtain a best fit to the differential cross-section data from these experiments; so, we have placed the results within quotation marks.

	herein	$\mathbb{P} + v_{cN}$	$\mathbb{P}$ -am.	GPD
GlueX	5.6	5.2	10.9	“6.0”
$J/\psi$ -007	7.8	9.7	5.1	“2.6”
All	7.0	8.1	7.2	“3.6”

# Model of Pomeron Exchange

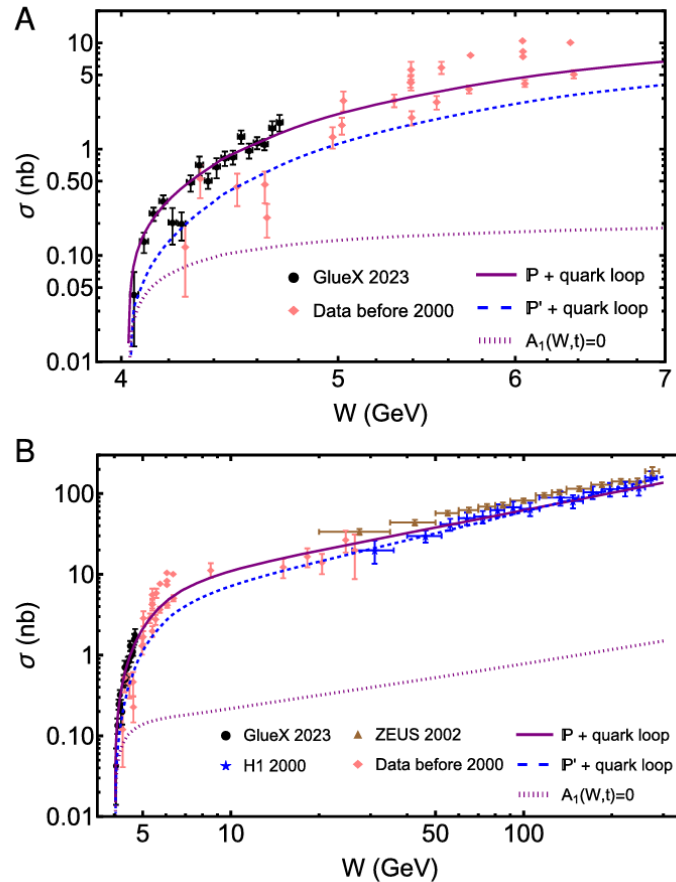


**Table 4**

$\chi^2/\text{dof}$  associated with selected reaction models when compared with data on different  $W$  (in GeV) ranges. Row 1:  $W < 5$  – [22,23, GlueX]. Row 2:  $W > 20$  – [31,32, H1, ZEUS]. Row 3: All  $W$  – [22,23, GlueX] and [31,32, H1, ZEUS]. Row 4 –  $W > 20$  – [31, H1] only. Row 5: All  $W$  – [22,23, GlueX] and [31, H1] only. The entry “undefined” highlights that the model cannot be applied beyond the near-threshold region. Ref. [32, ZEUS] reports a large uncertainty in  $W$ , but a small uncertainty in  $\sigma$ . This distorts the  $\chi^2$ ; so, the list also contains entries that exclude ZEUS from the  $\chi^2$  evaluation.

(GeV)	herein	$\mathbb{P} + v_{cN}$ [21]	$\mathbb{P}$ -am.	GPd [19]
$W < 5$	1.4	1.7	3.0	2.5
$W > 20$	5.7	2.8	5.3	undefined
All $W$	3.5	2.1	4.1	undefined
$W > 20_{H1}$	0.42	2.1	0.40	undefined
All $W_{H1}$	1.0	1.6	2.1	undefined

# arXiv:2210.02154

Eur. Phys. J. A manuscript No.  
(will be inserted by the editor)

## Models of $J/\Psi$ photo-production reactions on the nucleon

T.-S. H. Lee<sup>a,1</sup>, S. Sakinah<sup>b,2</sup>, Yongseok Oh<sup>c,2,3</sup>

<sup>1</sup>Physics Division, Argonne National Laboratory, Argonne, Illinois 60439, USA

<sup>2</sup>Department of Physics, Kyungpook National University, Daegu 41566, Korea

<sup>3</sup>Asia Pacific Center for Theoretical Physics, Pohang, Gyeongbuk 37673, Korea

Received: date / Accepted: date

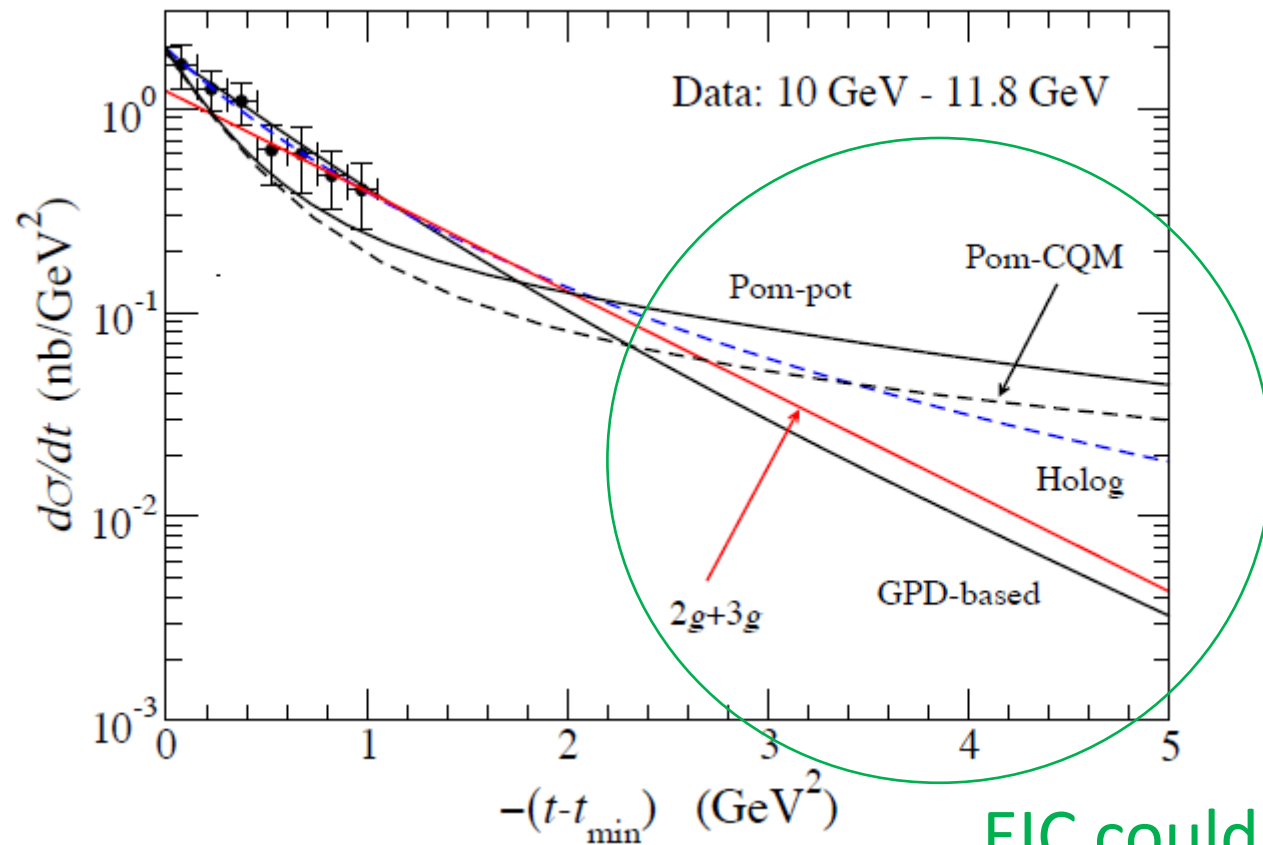
**Abstract** The  $J/\Psi$  photo-production reactions on the nucleon can provide information on the roles of gluons in determining the  $J/\Psi$ -nucleon ( $J/\Psi$ -N) interactions and the structure of the nucleon. The information on the  $J/\Psi$ -N in-

energies very near the  $J/\Psi$  production threshold. Possible improvements of the considered models are discussed.

5 Oct 2022



# t-dependence



EIC could help!

# Summary

- No signal of  $P_c(4440)$  in the energy dependence of total cross sections.
- Gluon exchange is speculated to dominate in the reaction of near-threshold  $J/\psi$  photoproduction. Within this picture, the differential cross sections  $d\sigma/dt$  could be used for the extraction of gravitational form factors,  $A$  and  $C$ , of the proton. The mass and scalar radius of protons are determined accordingly.
- Models of open-charm or Pomeron exchange are not ruled out by the data. Future EIC measurements of  $d\sigma/dt$  at large  $|t|$  could differentiate the correct modeling.